

Article

Performance of Eco-Friendly Zero-Cement Particle Board under Harsh Environment

Arman Hatami Shirkouh ¹, Farshad Meftahi ¹, Ahmed Soliman ^{1,*} , Stéphane Godbout ² and Joahnn Palacios ²

¹ Building Civil and Environmental Engineering, Gina Cody School of Engineering and Computer Science, Concordia University, Montreal, QC H3G 1M8, Canada; arman.hatamishirkouh@mail.concordia.ca (A.H.S.); farshad.meftahi@concordia.ca (F.M.)

² Research and Development Institute for the Agri-Environment (IRDA), Quebec, QC G1P 3W8, Canada

* Correspondence: ahmed.soliman@concordia.ca

Abstract: The increasing scarcity of virgin natural resources and the need for sustainable waste management in densely populated urban areas have heightened the importance of developing new recycling technologies. One promising approach involves recycling agricultural waste in construction applications and transforming it into secondary products. This is anticipated to reduce the demand for new resources and lower the environmental impact, aligning with industrial ecology principles. Combined with a low carbon emission binder (i.e., alkali-activated), utilizing agro-waste to produce zero-cement particle boards is a promising method for green construction. Traditionally, particle boards are engineered from wood or agricultural waste products that are pressed and bonded with a binder, such as cement or synthetic resins. However, alternative binders replace cement in zero-cement particle boards to address environmental concerns, such as the carbon dioxide emissions associated with cement production. This study investigated the effects of accelerated aging on the performance of alkali-activated agro-waste particle boards. Accelerated aging conditions simulate natural aging phenomena. Repeated wetting–drying and freezing–thawing cycles increased water absorption and thickness swelling and reduced flexural strength. The thermal performance of the alkali-activated particle boards did not exhibit significant changes. Hence, it was confirmed that agro-waste has a high potential for utilization in producing particle boards provided that the working environment is carefully selected to optimize performance.

Keywords: alkali-activated materials; agro-waste; particle board; swelling; accelerated aging conditions

check for
updates

Citation: Hatami Shirkouh, A.; Meftahi, F.; Soliman, A.; Godbout, S.; Palacios, J. Performance of Eco-Friendly Zero-Cement Particle Board under Harsh Environment. *Appl. Sci.* **2024**, *14*, 3118. <https://doi.org/10.3390/app14073118>

Academic Editors: Sandra Lucas and Guilherme Ascensão

Received: 20 February 2024

Revised: 30 March 2024

Accepted: 5 April 2024

Published: 8 April 2024



Copyright: © 2024 by the authors. Licensee MDPI, Basel, Switzerland. This article is an open access article distributed under the terms and conditions of the Creative Commons Attribution (CC BY) license (<https://creativecommons.org/licenses/by/4.0/>).

1. Introduction

Alkali-activated concrete provides a sustainable and innovative alternative to traditional Portland cement-based concrete [1]. Alkali-activated materials offer several advantages. They reduce carbon dioxide emissions associated with cement production by utilizing industrial by-products like fly ash and slag, which would otherwise be disposed of as waste and sent to landfills [2]. This makes them an environmentally friendly alternative. Additionally, alkali-activated materials demonstrate excellent durability, resistance to chemical attack, and reduced shrinkage compared to traditional concrete [3]. As a result, alkali-activated materials are distinguished from cement-based materials as they are considered sustainable, durable, and high-performance materials for various construction applications, contributing to the development of more environmentally conscious and long-lasting structures [4]. In this regard, alkali-activated materials are used for different applications. One of these applications is an alkali-activated particle board.

An alkali-activated particle board is a new product in the construction industry, bringing high durability and resistance to traditional particle boards [5]. This type of board is treated with alkali substances that enhance its performance characteristics, most notably its resilience against moisture and its potential for higher mechanical strength [6]. The process involves activating aluminosilicate materials using alkaline solutions, creating

chemical reactions that form durable bonds within the structure [7]. Mixing such binder with wood-based materials forms alkali-activated particle boards with improved environmental stability over cement-bonded particle boards, showing higher resistance to water absorption and less susceptibility to swelling or warping [5]. In addition, it presents an eco-friendly alternative due to its low-energy processes and potential for incorporating recycled materials [8].

Aras et al. explored the impact of incorporating olive mill solid waste (OSW) residue and different cement types on the properties of cement-bonded particle boards (CBPBs) [9]. In another study, Hou et al. investigated the fabrication of a value-added cement-bonded particle board (CBPB) using Masson pine processing residues and Portland cement. The results demonstrated good compatibility between Masson pine residues and cement, with higher cement/wood ratios leading to improved physical and mechanical properties in the CBPB [10]. Also, Odeyemi et al. investigated the utilization of agricultural wastes for producing cement-bonded particle boards, focusing on their physical and mechanical properties [11]. Ohijeagbon et al. developed composite ceiling boards bonded with cement using locally sourced wood residue from teak and African locust bean tree. The physico-mechanical properties were evaluated, including the moisture content, density, water absorption, drying shrinkage, and strength characteristics [12]. Bufalino et al. investigated the influence of the wood's chemical composition, anatomical traits, and density on the performance of cement-bonded particle boards (CBPBs); the research elucidates their impact on cement curing, the matrix–reinforcement interface, and the final CBPB's performance [13]. Another study by Faria et al. investigated the compressive behavior of cement-bonded particle board (CBPB) elements, aiming to expand its application to structural elements [14]. Using alkali-activated binders in particle board production as an alternative to cement has garnered attention due to their potential for enhancing performance and sustainability [5,15]. Researchers have explored different alkali-activated binders derived from industrial by-products and waste materials, evaluating their effects on alkali-activated particle boards' mechanical and physical properties [5]. Furthermore, efforts have been made to optimize manufacturing techniques, such as the particle size distribution and mixing parameters, to enhance the overall quality and performance of cement-bonded particle boards and alkali-activated particle boards [5,9]. These findings in the literature highlight the potential of cement-bonded particle boards and alkali-activated particle boards to be used as viable alternatives to conventional particle boards, paving the way for further advancements and practical applications in the construction industry.

Despite significant research progress regarding particle boards, several notable gaps remain in understanding their long-term durability and performance, particularly under harsh environmental conditions. Further exploration is needed to assess how particle boards withstand moisture, temperature fluctuations, and external stresses over time [16]. Moreover, while their mechanical properties have been studied, comprehensive research has not considered the effects of parameters like the particle size, binder composition, and manufacturing processes on the overall performance [11]. Additionally, there is limited investigation into the practical implementation of particle boards in real-world structural applications and their compatibility with other building materials. Also, a particle board is a cornerstone material in furniture manufacturing, renowned for its cost-effectiveness, versatility, and adaptability to a wide range of finishes and treatments. Predominantly utilized in producing flat-pack furniture, cabinets, shelving units, and countertops, a particle board's widespread application is a testament to its suitability for lightweight yet durable furniture designs. Its capacity to be engineered from recycled wood fibers aligns with contemporary sustainability trends, offering an eco-friendly alternative to solid wood. However, research on a particle board's long-term durability, particularly in environmental stressors such as moisture and temperature fluctuations, remains insufficient [17,18]. A deeper investigation into how various factors—such as the particle size, binder composition, and manufacturing techniques—affect its performance could reveal potential enhancements for its application

in not only furniture, but also in broader structural contexts, thereby bridging critical knowledge gaps in its use within the construction and furniture industries [19].

On the other hand, forecasts indicate the growth of agricultural production in the coming years. The purpose of these products is not only to provide food for the human population but also to meet industrial needs. Furthermore, agricultural commodities play a pivotal role in the textile industry by providing natural fibers such as cotton, flax, and hemp for manufacturing textiles and apparel [20]. The increasing growth of bioenergy from biofuel has been an example of the diversification of agricultural products in recent years. This is more evident in products with starch and cellulose [21]. In addition, agricultural plant residues have a special place as biomass and are considered to have good potential for green energy production [22]. In 2006, bioenergy accounted for about 10% of the world's energy [20]. The demand for crops experienced a significant upward trend from 2000 to 2015 due to the topic of biofuel production [23]. This demand is anticipated to produce a massive amount of agro-waste. Hence, the present study evaluates the possibility of utilizing agro-waste in producing alkali-activated particle boards and its effects on mechanical properties and durability under different curing conditions.

This research endeavors to revolutionize sustainable practices in the construction and agricultural sectors by utilizing agro-waste, waste reduction, and renewable resources. The primary aim is to develop a viable product, namely a zero-cement agro-waste particle board, that meets the rigorous technical standards of construction applications and delivers substantial economic and environmental benefits to the agricultural industry. By focusing on the production of a zero-cement particle board, this study aims to advance the understanding and application of alkali-activated particle board technology within engineered agro-waste composites. Through comprehensive experimentation and analysis, the findings of this research are expected to significantly contribute to the field, paving the way for the widespread adoption of sustainable alternatives in construction and agriculture.

2. Materials and Methods

Granulated blast furnace slag (hereafter called slag) was used as a binder for all zero-cement particle board mixtures with an average particle size of 14.5 μm . The physical and chemical properties of the slag are presented in Table 1. The dry-powder activator, sodium meta-silicate (Na_2SiO_3), with a 10% ratio, was mutually utilized to activate the zero-cement particle board mixtures. Na_2SiO_3 had a density of 1.09 g/cm^3 and a molar ratio of 1.0. The chemical and physical properties of the anhydrous sodium meta-silicate are shown in Table 2 in the manufacture datasheet. A water-to-binder (w/b) ratio of 0.40 was determined based on the mass of the binder. An agro-waste commercially known as Topimamerboor was used as an aggregate to produce zero-cement-bonded particle boards using 1:2, 1:3, and 1:4 ratios with respect to the binder. Figure 1 shows the agro-waste aggregate used in this study.

Table 1. Chemical compositions of used slag.

Items	SiO_2	Al_2O_3	CaO	Fe_2O_3	SO_3	MgO	K_2O	Na_2O	TiO_2	MnO_2
(%)	36.5	10.2	37.6	0.5	3.1	11.8	0.4	0.3	1.0	0.4

Table 2. Chemical and physical properties of anhydrous sodium meta-silicate.

Property	W_t % Na_2O	W_t % SiO_2	W_t % H_2O	Density (kg/m^3)	Particle Size	Melting Point ($^\circ\text{C}$)	Heat of Solution (kJ/mol)
Typical Data	50.5	46.2	<3	1090	93% in 20 to 65 mesh	1088	−31.7



Figure 1. Agro-waste used in this study (commercial name is Topimamerboor).

2.1. Mixture Procedure and Properties

In this study, three mixed designs were cast, as shown in Table 3. The agro-waste was submerged in water for 24 h to reduce its high-water absorption (saturation level) and then compressed with a hydraulic jack with 4 MPa of pressure before mixing. Afterward, the agro-waste was blended with other ingredients according to ASTM C305 [24] for 5 min. Due to the wet condition of the agro-waste, the water-to-binder ratios were set at approximately 0.4. The specimens were cast into molds and rested for 24 h at a temperature and relative humidity of 23 ± 2 °C and $50 \pm 3\%$, respectively. The molds were clipped on the top and bottom from two sides to prevent the elastic expansion of the agro-waste for the first 24 h.

Table 3. Mix properties of zero-cement particle boards.

Mix Code	W/B	Meta-Silicate (%)	Agro-Waste/Binder Ratio	Slag (g)	Water (g)
C200	0.4	10	1:2	200	80
C300	0.4	10	1:3	300	120
C400	0.4	10	1:4	400	160

C reflects the exposure and curing conditions. For ambient conditions: NC for 25 freeze–thaw cycles is 25FT; for 25 drying–wetting cycles: 25DW.

2.2. Exposure Conditions

After pressing, the compressed material was released, and the boards were removed from the mold. Three exposure conditions were applied after the specimen was cured for 28 days: ambient conditions, wetting and drying cycles, and freezing and thawing cycles.

2.2.1. Repeated Wetting and Drying

Repeated curing in wetting and drying conditions were performed with the aim of evaluating material degradation, including risks like cracking and spalling, and to compare the durability of different materials under standardized cyclic conditions of wetting and drying. First, to maintain stable environmental conditions and prevent water loss, the boards were covered within a closed box and kept in the laboratory for 28 days. For the wetting and drying curing condition, 25 wetting and drying cycles were conducted on specimens by alternating the temperature and relative humidity after 28 days of curing, as per ASTM C1185 [25]. Repeating the wetting and drying cycles could simulate the rain–heat cycles in natural weathering. Due to this aging condition, some fundamental chemical and physical deterioration mechanisms are stimulated. Moreover, these conditions increase the alkaline pore water, which is expected to attack the agro particles and the migration (through dissolution and re-precipitation) of some alkali-activated hydration products into the interfaces.

2.2.2. Modified Freezing and Thawing

This investigation examines the impact of repeated freezing–thawing cycles on product integrity, focusing on the potential for internal pressures and cracking caused by the expansion of water as it freezes within the capillary pores of cement paste. This study applied 25 freezing–thawing cycles to specimens of alkali-activated agro-waste particle boards following the same temperature and cycle mentioned in the ASTM C666 standards [26]. First, to maintain stable environmental conditions and prevent water loss, the boards were covered within a closed box and kept in the laboratory for 28 days. Before cycling, each specimen was submerged in water at less than 5 °C (41 °F) for 48 h. The specimens were then exposed to alternating cycles of freezing and thawing, fluctuating between 20 ± 3 °C (68 ± 5 °F), with each cycle comprising 16 h of freezing followed by 8 h of thawing.

2.3. Tests

2.3.1. Mass Loss

The change in the mass of tested specimens was used to indicate the particle boards' degradation after exposure to different conditions. The mass of each specimen was measured immediately after finishing curing and before exposure to assigned conditions, representing the initial mass. The mass was measured again after exposure to various numbers of cycles.

2.3.2. Density

Following BS EN 12390–7:2019 [27], the density of the samples was determined. Two specimens were cut out, and their weights were recorded based on their volumes. The bulk densities of the samples were calculated using Equation (1).

$$\text{Density (g/cm}^3\text{)} = W_a/V_a \quad (1)$$

where W_a = air-dried weight, and V_a = air-dried volume.

2.3.3. Water Absorption

Water absorption was determined according to BS 1881–122:2011 [28]. The initial weight was recorded using a weighing balance of two specimen samples cut from the board. The specimens were weighed after being immersed in water for 2 and 24 h (at room temperature), and the weight of each specimen was recorded as the final weight. Equation (2) was used to determine the percentage of water absorbed by each specimen.

$$\text{WaterAbsorption (\%)} = \frac{W_f - W_i}{W_i} \times 100 \quad (2)$$

where W_f = the final weight of the particle board; W_i = the initial weight of the particle board.

2.3.4. Thickness Swelling

The thickness swelling assessment was conducted per the specifications outlined in the ASTM standard D1037-03 [29]. Initial measurements of the samples' thicknesses were precisely recorded utilizing a Vernier caliper. Subsequently, the samples underwent immersion in water for 2 and 24 h, after which their final thickness measurements were taken. The quantification of water absorption for each sample, expressed as a percentage, was calculated using Equation (3), thereby facilitating the analysis of water-induced dimensional changes.

$$\text{ThicknessSwelling (\%)} = \frac{T_f - T_i}{T_i} \times 100 \quad (3)$$

where T_f = the final thickness of the particle board; T_i = the initial thickness of the particle board.

2.3.5. Thermal Performance

This test focused on assessing the thermal performance of concrete when exposed to radiant heat from a heat and cold cycle. Specimens with dimensions of $150 \times 150 \times 10$ mm from alkali-activated agro-waste particle boards were tested. The goal was to simulate the heat exposure that particle board surfaces might experience, with real-world conditions indicating a surface temperature of approximately 30°C . We aimed to better understand how heat penetrates particle boards, as it can significantly impact a building's indoor temperatures. The variations in the sample surface's temperature were monitored using a high-resolution camera forward-looking infrared (FLIR— 160×120 IR resolution) every 10 min. A thermocouple attached to a data logger was used to monitor the temperature inside the chamber (Figure 2). The heating and cooling cycle details are depicted in Figure 3.

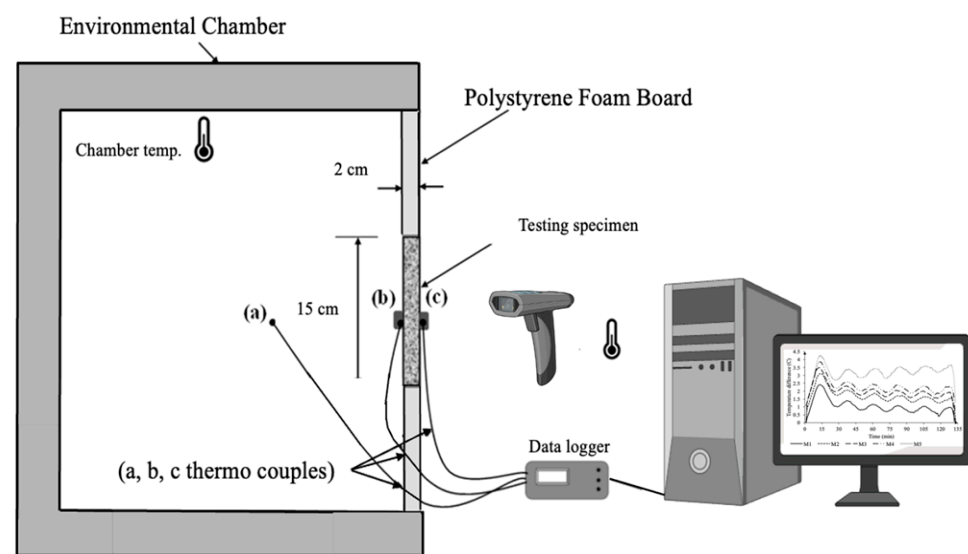


Figure 2. Schematic of heat transfer rate setup.

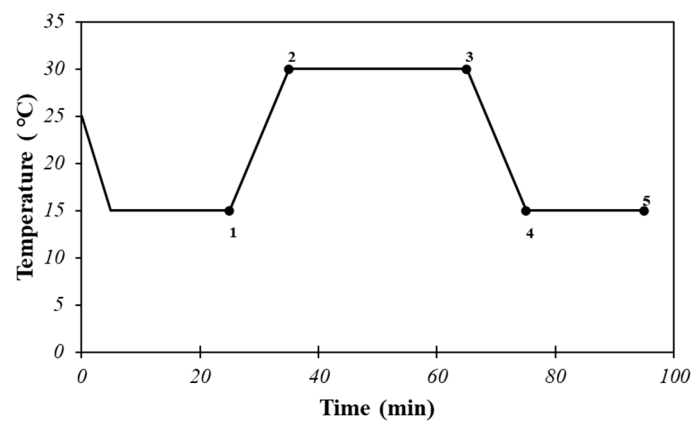


Figure 3. Thermal performance heating and cooling cycle and 5 monitoring points.

2.3.6. Flexural Strength

The flexural strength of the zero-cement particle board was determined based on ASTM D 1037 [29]. The particle boards were placed flat onto a flexural beam apparatus and subjected to a three-point loading setup, with the maximum load being recorded. The load was gradually applied until the particle boards failed, and a load versus deflection curve was plotted. The force that caused the particle board to fail was identified.

3. Results

3.1. Density

Figure 4 shows the result of the alkali-activated particle board density. The results show that specimen 25WD200 had the lowest density of 1052 kg/m^3 , and specimen NC400 had the highest density of 1691 kg/m^3 . According to IS 14276 [30], the suggested lower limit for density is 1250 kg/m^3 , while JIS.A.5908 [31] advocates for a minimum density value of 800 kg/m^3 . All manufactured particle boards adhered to these minimum standards as recommended. Figure 4 shows that the particle board density increases when the slag content increases. However, the density of the particle boards decreased when the specimens were exposed to the freezing and thawing cycles as well as the drying and wetting cycles. Also, the results show that the density of the particle boards decreased when the number of cycles increased. For instance, the density mixtures with 300 kg/m^3 of slag exposed to 10 FT cycles was 1486 kg/m^3 , while after 24 FT cycles, it was 1310 kg/m^3 . Also, the specimens cured under wetting and drying cycles had a lower density than those cured under freezing and thawing cycles. When comparing 25FT400 with 25WD400, it can be seen that it exhibited 8.5% less density. This is attributed to the change in the thickness of the particle board specimens when cured in the freezing and thawing cycles or wetting and drying cycles, as illustrated later.

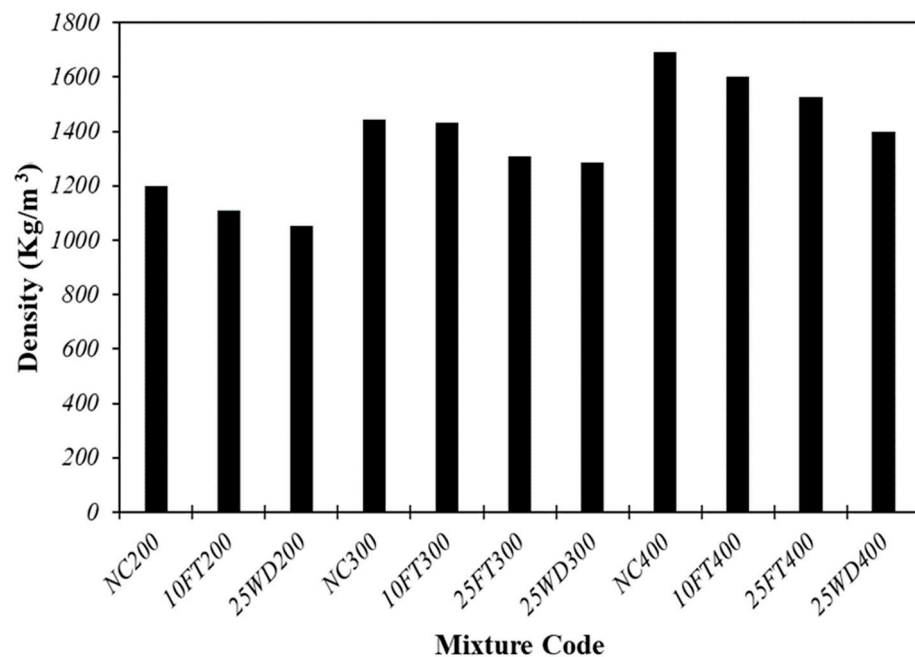


Figure 4. The density of the particle board with different slag contents and curing conditions.

3.2. Thickness Swelling

The thickness swelling of the alkali-activated particle board submerged in water for 2 and 24 h is illustrated in Figure 5. According to the guidelines set by the ASTM standard D1037-03 [29], the maximum allowable thickness swelling is 8%. As a result, all of the tested specimens met the requirement for thickness swelling. The results showed that 25FT200 and NC200 had the most significant changes in thickness, which were 5.12% and 4.65% after 24 h of submersion in water, respectively. However, the lowest change in thickness was exhibited by NC400, which was 2.17% after 2 h of submersion in water. This can be attributed to the ratio of agro-waste to slag, indicating that a higher slag content decreases thickness swelling. The widely accepted fact is that when the ratio of agro-waste to slag in particle boards rises, it leads to a notable increase in the thickness swelling, resulting in a decline in the boards' dimensional stability [11].

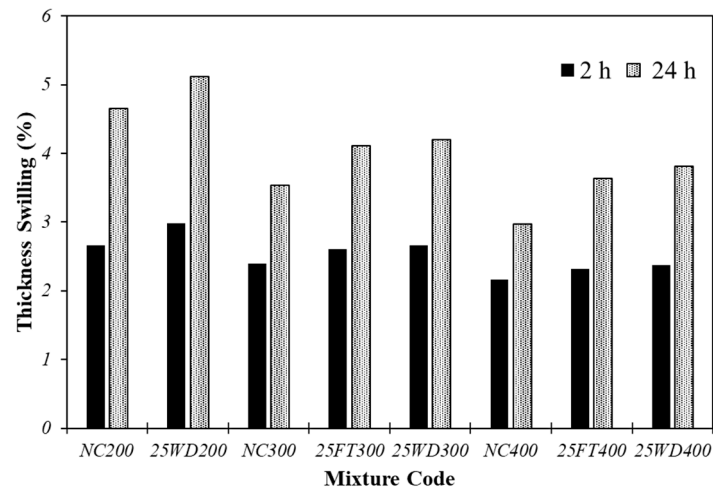


Figure 5. The result of the thickness swelling of the particle board with different slag contents and curing conditions.

On the other hand, the thickness swelling was increased when the particle boards were cured in freezing and thawing or drying and wetting conditions. For instance, it can be shown that specimens 25FT300 and 25WD300 had more changes in comparison with NC300, which were 4.11% and 4.20%, respectively. Also, it can be shown that curing in drying and wetting conditions has a greater effect than curing in freezing and thawing conditions. For instance, specimen 25WD400 had more thickness swelling changes than 25FT400. This can be attributed to the increase in the amount of pores when the specimens are cured in these conditions.

3.3. Water Absorption

The result of the water absorption test of the alkali-activated agro-waste particle boards is shown in Figure 6. The specimens were tested after being immersed in water for 2 and 24 h. The results show that the highest water absorption was achieved for 25WD200, which was about 46.88% after 24 h of water immersion. However, the lowest water absorption was achieved for NC400, at about 28.8%. Also, when the slag content increased in the particle board specimens, it decreased water absorption—for instance, NC200 achieved about 29.44% in 2 h of water immersion. However, the lowest water absorption was achieved for NC400, at about 24.35%. This can be attributed to the ratio of agro-waste to slag. After increasing the ratio of slag to agro-waste, the water absorption of the specimen of particle boards decreased due to a higher degree of hydration and the formation of hydration products that seal-coated the agro-waste particles. As shown in Figure 6, the particle board specimens had higher water absorption when immersed for 24 h than those immersed for 2 h. In addition, the specimens that were cured in drying–wetting and freezing–thawing conditions had higher water absorption than those in ambient curing conditions. For instance, 25WD400 had more water absorption than NC400. Also, the water absorption of the particle board specimens follows the order from low to high: ambient curing condition, wetting and drying cycle, and freezing and thawing cycle. This can be attributed to the reduction in the polymerization process and the formation of hydration products to seal coat the agro particles.

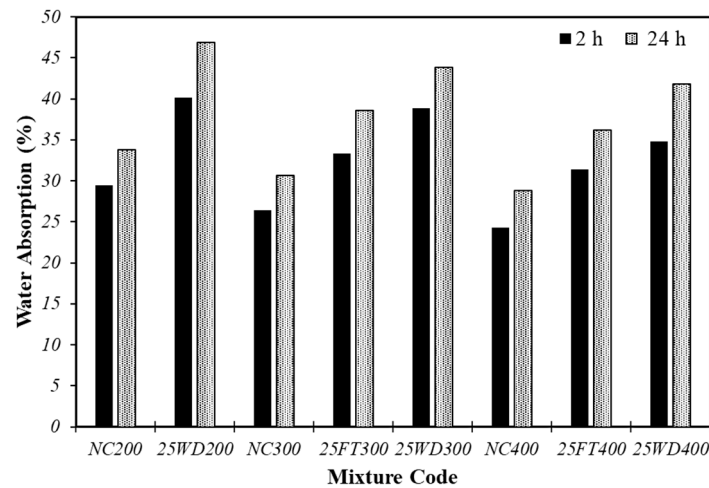


Figure 6. The result of the water absorption of the particle board with different slag contents and curing conditions.

3.4. Failure Mode

Figure 7 illustrates the failure modes of the alkali-activated particle boards and various degrees of damage. Obviously, the surfaces of all specimens exhibited rough textures, and there was an increase in the extent of corner loss in the specimens subjected to freezing–thawing cycles. For instance, considering the FT300 specimen as a representative, after 10 cycles, its surface underwent minimal alteration compared to the NC300 specimen. However, after 25 freezing–thawing cycles, the specimen’s surface became notably rougher. This was accompanied by the detachment of small mortars that fell off from the corners and the emergence of micro-cracks on the surface. Additionally, noticeable swelling was observed on the specimens’ surfaces due to agro-waste in the material composition. This swelling became more pronounced after 25 cycles of freezing and thawing conditions.

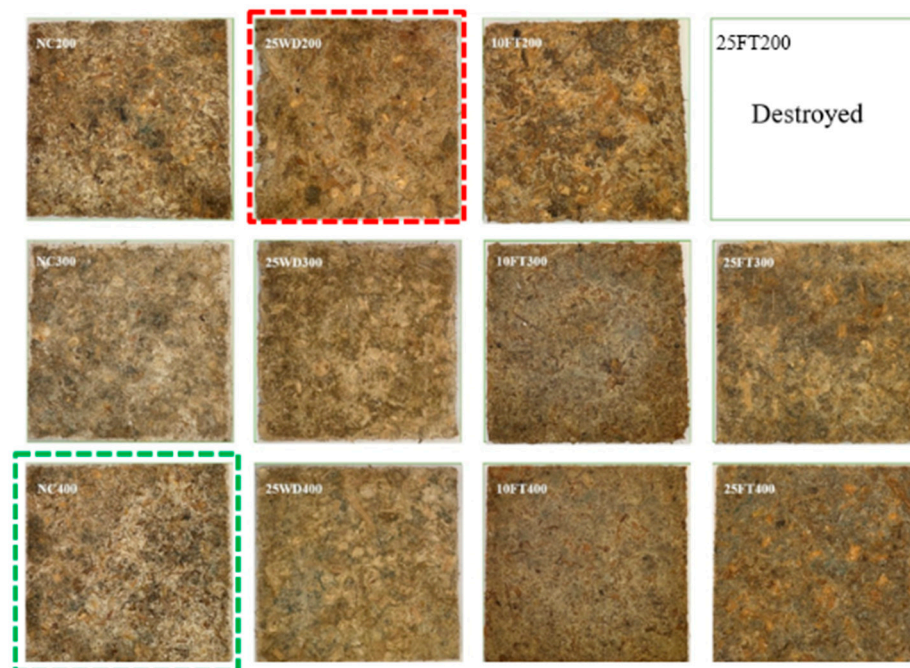


Figure 7. Failure rate of alkali-activated particle board specimens. (Destroyed: significant damage induced by exposure conditions, fail to parts).

Furthermore, the amount of slag content exerts a notable influence on the deterioration process of the specimens. At the same freezing–thawing cycles, it is evident that lower amounts of slag within the particle board specimens lead to more pronounced degradation. This trend is illustrated in Figure 7, where the NC400 specimen displayed negligible changes (Green Dashed). The specimen exhibits only slight swelling with no noticeable alterations. In contrast, the 25FT200 specimen experienced significant deterioration, while the 25FT300 and 25FT400 specimens demonstrated even less pronounced degradation when compared to the specimens subjected to standard curing conditions.

Upon the completion of 25 freezing–thawing cycles, discernible damage became apparent on the edges of the 25FT300 prismatic specimens. Furthermore, the edges of the 10FT300 specimens began to peel off following 10 freezing–thawing cycles. Remarkably severe surface damage was observed in the case of the 10FT200 and 25FT300 specimens. Notably, the mortar layer on the surface of the 25FT300 specimens had entirely dislodged, leaving the agro-waste aggregate exposed. The degradation of the 10FT200 specimen was even more pronounced, with substantial peeling of the concrete edges and wider cracks on the surface.

For the wetting and drying cycles, a higher content of slag was found to contribute to a reduced level of degradation in the particle board specimens, and this was similar to the trend observed during the freezing and thawing cycles. Figure 6 illustrates a discernible contrast in degradation severity between the 25WD200 (Red Dashed) and 25WD400 specimens. The amount of degradation witnessed during the wetting and drying cycles substantially exceeded that observed during the freezing and thawing cycles. For instance, the 25WD300 specimen showed more degradation than its freezing and thawing cycle counterpart, 25FT300. Upon closer examination, it became evident that after undergoing 25 cycles of curing under wetting and drying conditions, the surfaces of the specimens exhibited significant changes. The mortar layer underwent complete detachment, forming small pits, thereby exposing the agro-waste on the surface. Furthermore, at the edges of the specimens, severe peeling of the alkali-activated material occurred, resulting in wider cracks on the surface.

3.5. Mass Loss

Figures 8 and 9 illustrate the effects of freezing–thawing and wetting–drying cycles on mass loss. Generally, the particle board specimens under freezing–thawing or wetting–drying conditions exhibited mass loss. A consistent increase in mass loss was observed as the number of freezing–thawing and wetting–drying cycles increased. For instance, the FT300 specimen exhibited a more substantial mass loss after 25 cycles (i.e., 5.31%) than after exposure to 10 cycles (i.e., 3.94%), as shown in Figure 8.

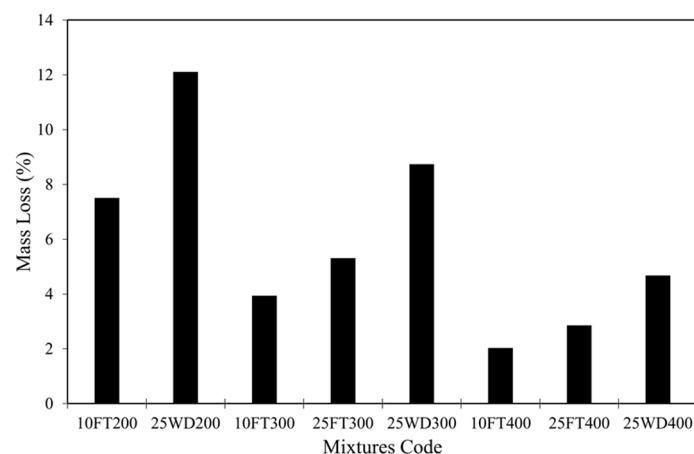


Figure 8. Effect of freezing–thawing and wetting–drying cycles on mass loss of agro-waste alkali-activated particle board.

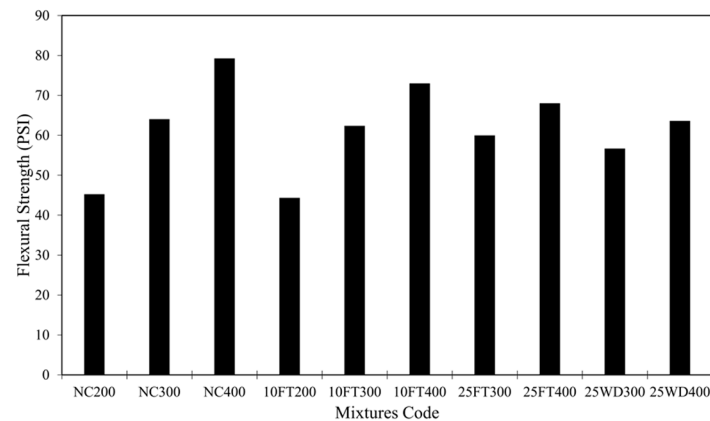


Figure 9. Effect of freezing–thawing and wetting–drying cycles on flexural strength of agro-waste alkali-activated particle board (1 Psi = 0.0069 MPa).

This observation can be attributed to the following rationales: In the initial phase, the expansion stress induced by freezing triggered specimen cracking. Consequently, a transfer of external water permeated internal voids and cracks, contributing to an augmented particle board specimen mass. However, as the freezing–thawing progressed, escalating freeze–thawing damage resulted in more degradation fragments from the specimen. This led to a reduction in the specimens’ mass. Subsequently, when the mass loss attributed to spalling surpassed the mass gain stemming from absorbed water, an overall decrease in the particle board specimen mass ensued, accentuating the magnitude of mass loss.

On the other hand, the 25WD200 specimen displayed the highest change in mass variations, amounting to approximately 12.11%. Additionally, the higher amount of slag in the specimen led to a lower percentage of mass loss. For example, 25WD200 had more mass loss than 25WD300 and 25WD400, which had 12.11%, 8.74%, and 4.68% mass losses, respectively. Moreover, it is notable that wetting–drying cycles exhibit a more significant degradation potential when compared to freezing–thawing curing conditions, even when considering an equivalent number of cycles, even at higher binder mixtures. The mass loss was 4.68% for 25WD400, while it was 2.86% for the 25FT400 specimen.

3.6. Flexural Strength

3.6.1. Flexural Strength in Repeated Wetting and Drying Cycles

Wetting–drying curing conditions were used to analyze the aging characteristics of the alkali-activated particle board. Flexural strength tests were carried out on an alkali-activated particle board under 25 cycles of repeated wetting–drying curing conditions. The impact of cyclic wetting–drying on the flexural behavior and results of the flexural tests, encompassing parameters such as strength and flexural load deflection, is graphically shown in Figure 10 and Figure 11, respectively.

Generally, the repeated wetting–drying cycles resulted in decreased flexural strength. The flexural performance of the alkali-activated particle board under wetting–drying curing conditions typically declined compared to the specimens that underwent standard curing conditions. For instance, the 25WD200 particle board specimen experienced more pronounced degradation, resulting in a complete loss of flexural strength. In contrast, the NC 200 variant exhibited a flexural strength of 42.24 Psi (0.29 MPa). The results were better with an agro-waste/slag ratio of 0.25 compared to 0.5. For instance, the flexural strengths of 25WD300 and 25WD400 are about 56 Psi (0.38 MPa) and 63 Psi (0.43 MPa), respectively. Moreover, for the same deflection value, mixtures exposed to freezing and thawing cycles sustained lower loads. This finding reflects the internal degradation and assassinated damage induced by wetting and drying cycles.

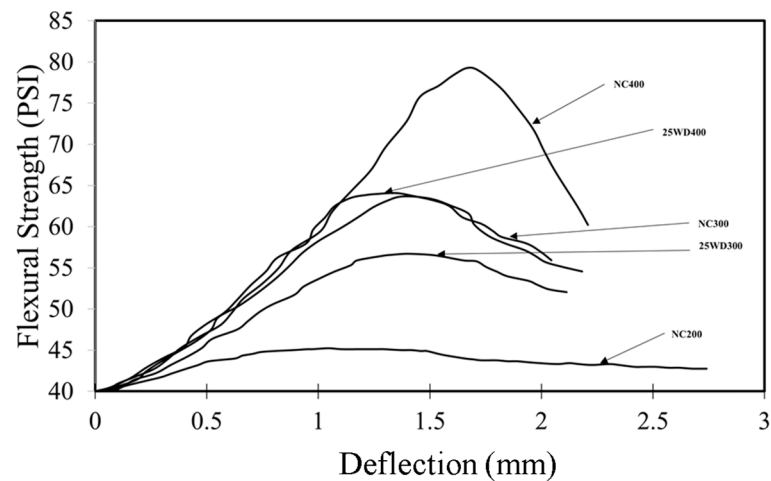


Figure 10. Effects of wetting–drying cycles on flexural curve characteristics of alkali-activated particle board (1 Psi = 0.0069 MPa).

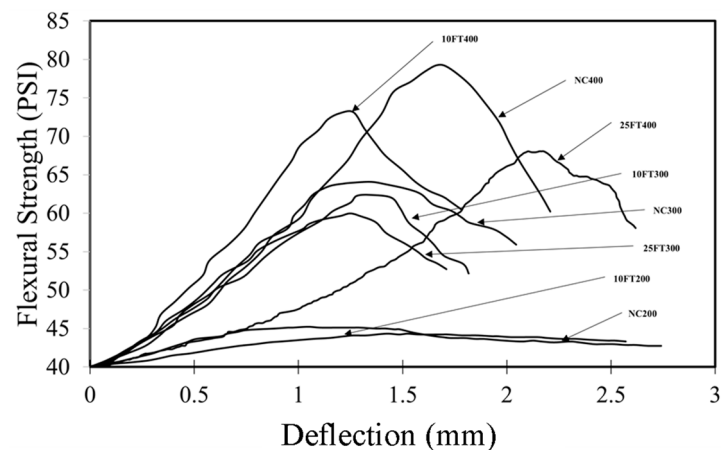


Figure 11. Effects of freezing–thawing cycles on flexural curve characteristics of alkali-activated particle board (1 Psi = 0.0069 MPa).

3.6.2. Flexural Strength in Freezing and Thawing Cycle

Freezing–thawing curing conditions were used to analyze the aging characteristics of the alkali-activated particle board. Flexural strength tests were performed on an alkali-activated particle board under 10 and 25 cycles of freezing and thawing curing conditions. The impact of cyclic freezing–thawing on the flexural behavior and results of the flexural tests, encompassing parameters such as strength, flexural load, and deflection, is graphically shown in Figure 10 and Figure 11, respectively.

Generally, the freezing and thawing curing conditions resulted in a decreasing trend for flexural strength. The flexural performance of the alkali-activated particle board under freezing–thawing curing conditions typically declined compared to the specimens that underwent standard curing condition. For instance, the 25FT200 particle board specimen experienced a complete loss of flexural strength. In contrast, the NC 200 variant exhibited a flexural strength of 42.24 Psi (0.29 MPa). Moreover, the results showed that increasing the number of cycles from 10 to 25 reduced the flexural strength more. For instance, the FT300 particle board specimen had a flexural strength of 62.3 Psi (0.43 MPa) after 10 cycles of freezing and thawing, while it exhibited a flexural strength of 59.9 Psi (0.41 MPa) after 25 cycles. The results were better at a lower agro-waste content. For instance, the flexural strengths of FT300 and FT400 are about 59.9 Psi (0.41 MPa) and 70 Psi (0.48 MPa), respectively.

3.7. Thermal Performance

All particle board specimens' surfaces were exposed to various temperatures as the environmental chamber's temperature was changed. The specimens were exposed to a 15 °C temperature for 25 min from an ambient temperature. Then, the specimens were exposed to a temperature of 30 °C for 30 min. Then, the temperature was lowered to 15 °C over 10 min and kept for 20 min. The result of the thermal performance of the alkali-activated agro-waste particle board is shown in Figure 12. It shows the temperature changes over time from the surface of the alkali-activated particle board specimens. The results show that using higher amounts of slag in the particle board specimens led to higher temperatures on the surfaces of the specimens. For example, the surface temperature of NC400 in all monitoring periods was much higher than that of NC200. Also, wetting–drying and freezing–thawing curing conditions followed the same trend as the ambient curing conditions. However, as shown in Figure 12, the wetting–drying and freezing–thawing curing conditions negatively affected the thermal performance of the alkali-activated particle board. The thermal performance when the specimens were cured under the wetting–drying or freezing and thawing curing conditions did not significantly change. For instance, 25FT300 and 25WD300 showed slightly lower temperatures than NC300. Also, the wetting–drying curing condition had a slightly lower temperature than the freezing and thawing curing condition. This can be attributed to two compensation effects: damage creating air gaps and a high water content. The thermal insulation induced by air gaps developed due to cracking and damage is compensated by the high water content and, consequently, higher thermal conductivity for the specimens.

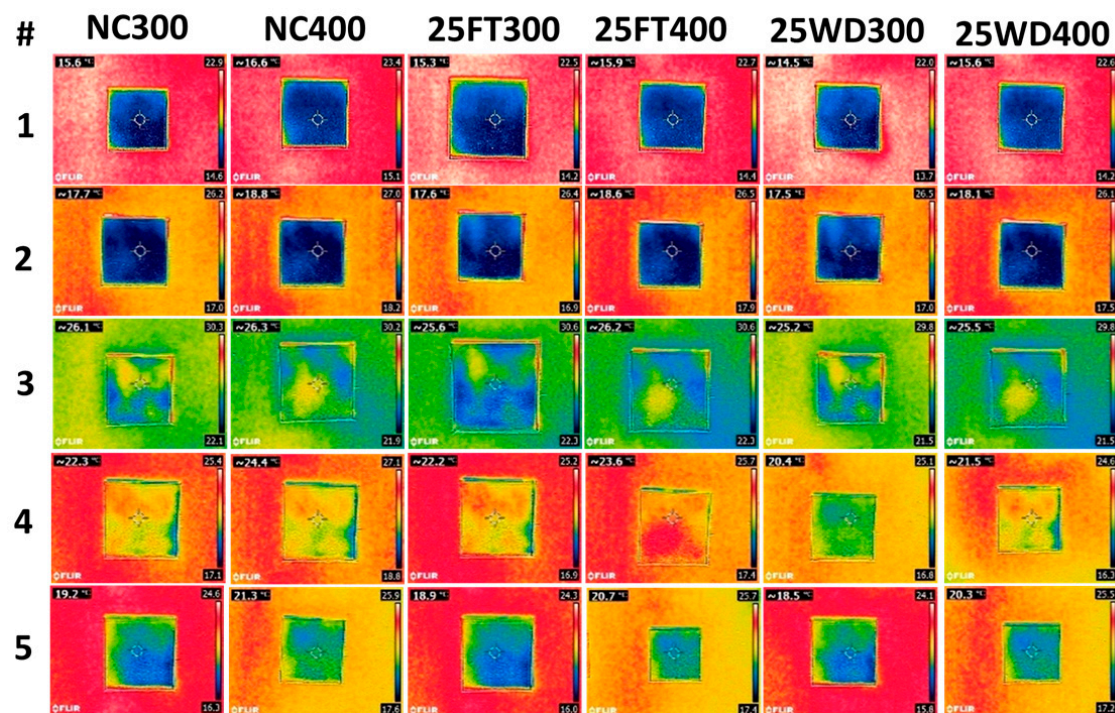


Figure 12. Result of thermal performance of alkali-activated agro-waste particle boards.

4. Conclusions

This study examined the effects of aging on the characteristics of an alkali-activated agro-waste particle board composite. Based on the findings and discussion presented, it can be firmly concluded that utilizing agricultural waste to produce alkali-activated particle boards is feasible but requires more caution when selecting the exposure conditions. Additionally, the influence of varying slag amounts was assessed, with the general trend

showing that increasing the slag content resulted in a higher flexural strength. The key observations from the test results include the following:

- A high binder content compensates for the high water absorption of agro-waste.
- Repeated wetting–drying curing conditions and freezing–thawing cycles led to a decreased flexural strength over time.
- Repeated wetting–drying curing conditions had a higher degradation impact than that induced by freezing–thawing cycles.
- Agricultural waste exhibited a lower specific gravity, resulting in a more porous structure and lower product density during curing.
- From a practical perspective, the ratio of agricultural waste to slag and its effect on flexural strength was relatively high.
- The exposure conditions greatly affected the thermal performance based on the degree of damage and water content induced.

Author Contributions: Conceptualization, A.S.; methodology, F.M. and A.S.; validation, A.H.S. and A.S.; formal analysis, A.H.S.; investigation, A.H.S.; resources, A.S., S.G. and J.P.; data curation, A.H.S.; writing—original draft preparation, A.H.S.; writing—review and editing, A.S.; visualization, A.H.S.; supervision, A.S.; project administration, A.S., S.G. and J.P.; funding acquisition, A.S. All authors have read and agreed to the published version of the manuscript.

Funding: This research was funded by the Natural Sciences and Engineering Research Council of Canada, Discovery Funding program, grant number RGPIN-2018-05094.

Institutional Review Board Statement: Not applicable.

Informed Consent Statement: Not applicable.

Data Availability Statement: All data are available in Arman Hatami Shirkouh Master thesis available at Concordia Lib. Website.

Acknowledgments: The authors would like to thank Lafarge for donating the slag and Institut de recherche et de développement en agroenvironnement (IRDA) for donating the agriculture waste.

Conflicts of Interest: The authors declare no conflicts of interest.

References

1. Valente, M.; Sambucci, M.; Chougan, M.; Ghaffar, S.H. Reducing the emission of climate-altering substances in cementitious materials: A comparison between alkali-activated materials and Portland cement-based composites incorporating recycled tire rubber. *J. Clean. Prod.* **2022**, *333*, 130013. [\[CrossRef\]](#)
2. Huseien, G.F.; Hamzah, H.K.; Sam, A.R.; Khalid, N.H.; Shah, K.W.; Deogrescu, D.P.; Mirza, J. Alkali-activated mortars blended with glass bottle waste nanopowder: Environmental benefit and sustainability. *J. Clean. Prod.* **2020**, *243*, 118636. [\[CrossRef\]](#)
3. Mohamed, O.A. A review of durability and strength characteristics of alkali-activated slag concrete. *Materials* **2019**, *12*, 1198. [\[CrossRef\]](#) [\[PubMed\]](#)
4. Provis, J.L. Alkali-activated materials. *Cem. Concr. Res.* **2018**, *114*, 40–48. [\[CrossRef\]](#)
5. Kuqo, A.; Mayer, A.K.; Amiandamhen, S.O.; Adamopoulos, S.; Mai, C. Enhancement of physico-mechanical properties of geopolymer particle-boards through seagrass fibres. *Constr. Build. Mater.* **2023**, *374*, 130889. [\[CrossRef\]](#)
6. Thi, K.-D.T.; Liao, M.-C.; Vo, D.-H. The characteristics of alkali-activated slag-fly ash incorporating the high volume wood bottom ash: Mechanical properties and microstructures. *Constr. Build. Mater.* **2023**, *394*, 132240.
7. Athira, V.S.; Charitha, V.; Athira, G.; Bahurudeen, A. Agro-waste ash based alkali-activated binder: Cleaner production of zero cement concrete for construction. *J. Clean. Prod.* **2021**, *286*, 125429. [\[CrossRef\]](#)
8. Ghanad, D.A.; Soliman, A. Bio-based alkali-activated controlled low strength material: Engineering properties. *Constr. Build. Mater.* **2021**, *279*, 122445. [\[CrossRef\]](#)
9. Aras, U.; Kalaycioğlu, H.; Yel, H.; Kuştaş, S. Utilization of olive mill solid waste in the manufacturing of cement-bonded particle-board. *J. Build. Eng.* **2022**, *49*, 104055. [\[CrossRef\]](#)
10. Hou, J.; Jin, Y.; Che, W.; Yu, Y. Value-added utilization of wood processing residues into cement-bonded particle-boards with admirable integrated performance. *Constr. Build. Mater.* **2022**, *344*, 128144. [\[CrossRef\]](#)
11. Odeyemi, S.O.; Abdulwahab, R.; Adeniyi, A.G.; Atoyebi, O.D. Physical and mechanical properties of cement-bonded particle board produced from African balsam tree (*Populus balsamifera*) and periwinkle shell residues. *Results Eng.* **2020**, *6*, 100126. [\[CrossRef\]](#)

12. Ohijeagbon, I.O.; Bello-Ochende, M.U.; Adeleke, A.A.; Ikubanni, P.P.; Samuel, A.A.; Lasode, O.A.; Atoyebi, O.D. Physico-mechanical properties of cement bonded ceiling board developed from teak and African locust bean tree wood residue. *Mater. Today Proc.* **2021**, *44*, 2865–2873. [[CrossRef](#)]
13. Bufalino, L.; de Souza, T.M.; Lima, N.N.; de Sá, V.A.; Tonoli, G.H.; Ferreira, C.A.; Junior, H.S.; de Sousa, R.B.; Zidanés, U.L.; de Paula Protásio, T.; et al. Contrasting the significant characteristics of pinewood and Amazon hardwoods to provide high-quality cement-bonded particle-boards. *Constr. Build. Mater.* **2023**, *394*, 132219. [[CrossRef](#)]
14. Faria, G.; Chastre, C.; Lúcio, V.; Nunes, Â. Compression behaviour of short columns made from cement-bonded particle board. *Constr. Build. Mater.* **2013**, *40*, 60–69. [[CrossRef](#)]
15. Olayiwola, H.O. *Development of Geopolymer Bonded Wood Composites*; Stellenbosch University: Stellenbosch, South Africa, 2021.
16. Soroushian, P.; Won, J.-P.; Hassan, M. Durability and microstructure analysis of CO₂-cured cement-bonded wood particle-board. *Cem. Concr. Compos.* **2013**, *41*, 34–44. [[CrossRef](#)]
17. El-Sayed, G.; Atallah, M.M.; Ahmad, M. Production of Fire-Resistant Particle Boards from some Agricultural Residues. *J. Soil Sci. Agric. Eng.* **2021**, *12*, 145–151. [[CrossRef](#)]
18. Ferrandez-García, C.C.; García-Ortuño, T.; Ferrandez-García, M.T.; Ferrandez-Villena, M.; García, C.E. Fire-resistance, physical, and mechanical characterization of binderless rice straw particle-boards. *BioResources* **2017**, *12*, 8539–8549. [[CrossRef](#)]
19. Emmanuel, O.U.; Kuqo, A.; Mai, C. Non-conventional mineral binder-bonded lignocellulosic composite materials: A review. *BioResources* **2021**, *16*, 4606. [[CrossRef](#)]
20. Hazell, P.; Pachauri, R.K. *Bioenergy and Agriculture: Promises and Challenges*; IFPRI: Washington, DC, USA, 2006.
21. Food and Agriculture Organization of the United Nations. *The State of Food and Agriculture 2008*; Food and Agriculture Organization of the United Nations: Rome, Italy, 2008; 128p.
22. UN Energy. *A Decision Support Tool for Sustainable Bioenergy*; Prepared by FAO and UNEP for UN Energy; UN Energy: New York, NY, USA, 2010.
23. ERCD-FAO Agricultural Outlook. *OECD-FAO Agricultural Outlook 2017–2026*; ERCD-FAO Agricultural Outlook: Rome, Italy, 2017; Volume 2026.
24. *ASTM C305*; Standard Practice for Mechanical Mixing of Hydraulic Cement Pastes and Mortars of Plastic Consistency. ASTM International: West Conshohocken, PA, USA, 2006.
25. *ASTM C1185*; Standard Test Methods for Sampling and Testing Non-Asbestos Fiber-Cement Flat Sheet, Roofing and Siding Shingles, and Clapboards. ASTM International: West Conshohocken, PA, USA, 2016.
26. *ASTM C666*; Standard Test Method for Resistance of Concrete to Rapid Freezing and Thawing. ASTM International: West Conshohocken, PA, USA, 2017.
27. *BS EN 12390-7*; Testing Hardened Concrete-Density of Hardened Concrete. British-Adopted European Standard; BSI: London, UK, 2019.
28. *BS 1881-122:2011*; Testing Concrete. Method for Determination of Water Absorption. British-Adopted European Standard; BSI: London, UK, 2011.
29. *ASTM D1037-12*; Standard Test Methods for Evaluating Properties of Wood-Base Fiber and Particle Panel Materials. ASTM International: West Conshohocken, PA, USA, 2012.
30. *IS 14276*; Cement Bonded Particle Boards—Specification. Bureau of Indian Standards: Old Delhi, India, 1995.
31. *JIS A 5908*; Particle-Board. Japanese Industrial Standard/Japanese Standards Association: Tokyo, Japan, 2022.

Disclaimer/Publisher’s Note: The statements, opinions and data contained in all publications are solely those of the individual author(s) and contributor(s) and not of MDPI and/or the editor(s). MDPI and/or the editor(s) disclaim responsibility for any injury to people or property resulting from any ideas, methods, instructions or products referred to in the content.